Thermal Decomposition of Trifluoromethoxycarbonyl Peroxy Nitrate, $CF_3OC(O)O_2NO_2$

MARTÍN D. MANETTI, FABIO E. MALANCA, GUSTAVO A. ARGÜELLO

INFIQC, *Departamento de Fisicoquímica, Facultad de Ciencias Químicas, Universidad Nacional de Córdoba, Ciudad Universitaria*, 5000 *Córdoba, Argentina*

Received 28 March 2007; revised 20 September 2007, 14 February 2008; accepted 26 March 2008

DOI 10.1002/kin.20355
Published online in Wiley InterScience (www.interscience.wiley.com).

ABSTRACT: The thermal decomposition of trifluoromethoxycarbonyl peroxy nitrate, $CF_3OC(O)O_2NO_2$, has been studied between 278 and 306 K at 270 mbar total pressure using He as a diluent gas. The pressure dependence of the reaction was also studied at 292 K between 1.2 and 270 mbar total pressure. The rate constant reaches its high-pressure limit at 70 mbar. The first step of the decomposition leads to $CF_3OC(O)O_2$ and NO_2 formation, that is, $CF_3OC(O)O_2NO_2 + M \leftrightarrows CF_3OC(O)O_2 + NO_2 + M$ (k_1, k_{-1}). Reaction (−1) was prevented by adding an excess of NO that reacts with the peroxy radical intermediate and leads to carbonyl fluoride (CF_2O), carbon dioxide (CO_2), nitrogen dioxide (NO_2), and small quantities of $CF_3OC(O)O_2C(O)OCF_3$. The kinetics of reaction (1) was determined by following the loss of $CF_3OC(O)O_2NO_2$ via IR spectroscopy. The temperature dependence of the decomposition follows the equation $k_1(T) = 1.0 \times 10^{16}\, e^{-((111\pm3)/(RT))}$ for the exponential term expressed in kJ mol^{-1}. The values obtained for the kinetic parameters such as k_1 at 298 K, the activation energy (E_a), and the preexponential factor (A) are compared with literature data for other acyl peroxy nitrates. The atmospheric thermal stability of $CF_3OC(O)O_2NO_2$ and its dependence with altitude is discussed. © 2008 Wiley Periodicals, Inc. Int J Chem Kinet 40: 831–838, 2008

INTRODUCTION

Peroxy nitrates (RO_2NO_2) are important species in the atmosphere because they act as reservoirs of NO_2 and RO_2 radicals. In particular, acyl peroxy nitrates ($R'C(O)O_2NO_2$) are relatively stable. Their atmospheric thermal lifetimes (from 1 h to several days) [1] are sufficiently long that they can be transported from their sources to remote places or to the stratosphere [2–4].

Peroxy acetyl (PAN; $CH_3C(O)O_2NO_2$), peroxy propionyl ($C_2H_5C(O)O_2NO_2$), and peroxy benzoyl ($C_6H_5C(O)O_2NO_2$) nitrates have been detected and measured in the atmosphere [5,6]. These compounds are formed in the troposphere as oxidation products of emitted hydrocarbons.

Industrial fluorinated compounds such as chlorofluorocarbons, hydrochlorofluorocarbons, hydrofluorocarbons, and hydrofluoroethers (CFCs, HCFCs,

Correspondence to: Gustavo A. Argüello; e-mail:gaac@fcq.unc.edu.ar.

Contract grant sponsor: Consejo Nacional de Investigaciones Científicas y Técnicas.
Contract grant sponsor: Secretaría de Ciencia y Técnica-UNC.
Contract grant sponsor: Fondo para la Investigación Científica y Tecnológica.

HFCs, and HFEs, respectively) lead to the formation of various fluorinated peroxy acyl nitrates in the atmosphere, for example, fluorocarbonyl ($FC(O)O_2NO_2$), trifluoroacetyl (FPAN; $CF_3C(O)O_2NO_2$), and trifluoromethoxicarbonyl ($CF_3OC(O)O_2NO_2$) peroxy nitrates [7].

Christensen et al. [8] determined the thermal stability of trifluoromethoxycarbonyl peroxy nitrate at 295.8 K in a mixture containing NO_2 and NO inside a smog chamber. von Ahsen et al. [7] synthesized the pure peroxy nitrate in bulk quantities and characterized the molecule (vapor pressure, boiling, and melting points, UV cross sections, IR and Raman spectra, NMR, etc.). In this paper, we present the study of the thermal decomposition of $CF_3OC(O)O_2NO_2$:

$$CF_3OC(O)O_2NO_2 + M \rightarrow CF_3OC(O)O_2 + NO_2 + M \quad (1)$$

in the presence of excess NO. As will be discussed later, the NO removes $CF_3OC(O)O_2$ radicals and thus prevents the back reaction with NO_2 to re-form the peroxy nitrate:

$$CF_3OC(O)O_2 + NO_2 + M \rightarrow CF_3OC(O)O_2NO_2 + M \quad (-1)$$

This allows us to isolate the forward reaction and study its kinetics.

EXPERIMENTAL

Chemicals

Commercially available samples of perfluoroacetic anhydride $(CF_3C(O))_2O$ (PCR), CO (PRAXAIR), NO, helium, and O_2 (AGA) were used. Oxygen was first condensed by flowing it at atmospheric pressure through a trap immersed in liquid air. It was then pumped under vacuum several times and transferred to a glass bulb while the trap was still immersed in liquid air. The NO_2 needed to synthesize the peroxy nitrate was prepared by reaction of NO samples with O_2 to finally form a mixture (ratio 1:10) of NO_2/O_2. $CF_3OC(O)O_2NO_2$ was synthesized by mixing, in a glass bulb $CF_3OC(O)O_3C(O)OCF_3$ (from laboratory samples previously synthesized in our group [9] with the NO_2/O_2 mixture. The trioxide slowly decomposes at subambient temperatures leading to $CF_3OC(O)O_2$ radical formation, which in the presence of NO_2 forms the nitrate as is described in von Ahsen et al. [7]. The purity of the trioxide and the peroxy nitrate was checked by comparison of the actual IR spectrum with known references. All the information about concentrations of species and their temporal variations comes from the recording of IR spectra. In all cases, they were taken with a Bruker IFS 66v FTIR with a 2-cm^{-1} resolution. Typically eight interferograms were coadded. For kinetic measurements, the spectra were recorded at 120 s intervals.

Methods

To measure the thermal decomposition and its temperature dependence, a double-walled IR gas cell (optical path 21 cm) was loaded with the peroxy nitrate samples and placed in the optical path of the IFS 66v FTIR spectrometer. To prevent the condensation of water in the windows cell, a homemade cell holder was constructed to allow the FTIR sample cavity to be evacuated. The temperature was regulated to within ± 1 K between 306 and 278 K using a Lauda cryostat. The kinetic measurements were carried out by following the disappearance of $CF_3OC(O)O_2NO_2$ through absorption peaks at 1760 and 1165 cm^{-1}, and the appearance of products (CF_2O at 1956 cm^{-1}, CO_2 and NO_2, using the integrated absorption bands, and $CF_3OC(O)O_2C(O)OCF_3$, which appears only in minor quantities at 1133 cm^{-1}).

RESULTS AND DISCUSSION

Thermal Decomposition and Kinetic Mechanism

As mentioned before, the thermal decomposition of $CF_3OC(O)O_2NO_2$ leads to the formation of NO_2 and $CF_3OC(O)O_2$ radicals [7]

$$CF_3OC(O)O_2NO_2 + M \rightarrow CF_3OC(O)O_2 + NO_2 + M \quad (1)$$

that in the absence of radical trapping species recombine to maintain the dissociation equilibrium through

$$CF_3OC(O)O_2 + NO_2 + M \rightarrow CF_3OC(O)O_2NO_2 + M \quad (-1)$$

At 298 K, the disappearance of $CF_3OC(O)O_2NO_2$ is slow (approximately 0.2% in 1 h) and drastically increases ($\sim$70%) in the presence of added NO.

The rate constant for reaction (k_{-1}) has not been previously reported, but it seems reasonable to assume that it will be similar to the analogous reaction of $CF_3C(O)O_2$ radicals

$$CF_3C(O)O_2 + NO_2 \rightarrow CF_3C(O)O_2NO_2 \quad (2)$$

which is temperature dependent and can be expressed as $k_2 = 6.6 \times 10^{-12}\ (T/298)^{-1}$ cm^3 $molecule^{-1}$ s^{-1} [10,11].

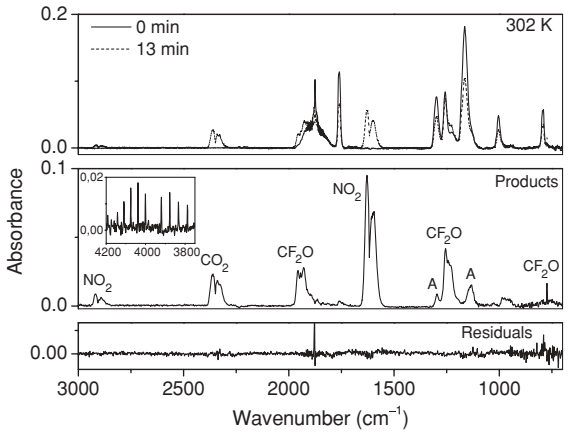

Figure 1 Infrared spectra of reactants (solid line) and reaction mixture after 13 min of thermal decomposition at 302 K (dashed line) are depicted in the upper plot. The middle plot shows the difference of the two spectra, where the solid line spectrum has been scaled by a factor corresponding to the degree of decomposition. The peaks are assigned to products as noted; "A" corresponds to $CF_3OC(O)O_2C(O)OCF_3$. The lower plot presents the residual spectrum that shows there are no complications with the subtraction.

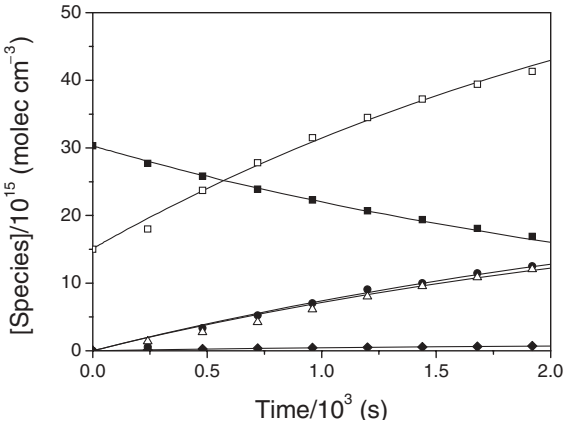

Figure 2 Experimental concentration–time profiles for $CF_3OC(O)O_2NO_2$ and products (symbols) and the fits obtained (lines) by integration of the kinetic model presented in Table I for a temperature of 298 K. ■ = $CF_3OC(O)O_2NO_2$; □ = NO_2; △ = CF_2O; ● = CO_2; ♦ = $CF_3OC(O)O_2C(O)OCF_3$.

The addition of excess NO removes $CF_3OC(O)O_2$ radicals in a way similar to that found for other peroxy radicals [8,12]

$$CF_3OC(O)O_2 + NO \rightarrow CF_3OCOO + NO_2 \qquad (3)$$

and prevents reaction (−1) from taking place. Arguments similar to those used for reaction (−1) can be used here to assume that the rate constant for reaction (3) will be similar to the rate constant of reaction (4)

$$CF_3C(O)O_2 + NO \rightarrow CF_3COO + NO_2 \qquad (4)$$

where $k_4 = 4.0 \times 10^{-12}\ e^{(563/T)}$ cm^3 molecule^{-1} s^{-1} is taken from Maricq et al. [13].

The upper plot of Fig. 1 shows the IR spectra of the reactants ($CF_3OC(O)O_2NO_2$ (0.8 mbar) and NO (3.2 mbar) 270 mbar total pressure) at $t = 0$, and the mixture of reactants and products after 13 min of reaction at 302 K. It is clearly visible the disappearance of $CF_3OC(O)O_2NO_2$ (peaks at 1760 and 1165 cm^{-1}, also used for quantification) and the concomitant appearance of products. The middle plot of Fig. 1 corresponds to the spectrum obtained after subtraction of reactants ($CF_3OC(O)O_2NO_2$ and NO) from the mixture spectrum and reveals the formation of CO_2, CF_2O, and NO_2 as the main products, together with a small quantity of $CF_3OC(O)O_2C(O)OCF_3$ and HF (see inset). Figure 2 shows the temporal variation in the concentration of the carbon-containing species. The appearance of the IR spectrum in Fig. 1 could lead to the misinterpretation that the contribution of $CF_3OC(O)O_2C(O)OCF_3$ is important if only the height of the bands is considered. This product is expected to form via the recombination of CF_3OCOO radicals (reaction (5)):

$$2CF_3OCOO \rightarrow CF_3OC(O)O_2C(O)OCF_3 \qquad (5)$$

and not by the recombination of peroxy radicals $CF_3OC(O)O_2$ (reaction (6)):

$$2CF_3OC(O)O_2 \rightarrow CF_3OC(O)O_2C(O)OCF_3 + O_2 \qquad (6)$$

since they are efficiently captured by the NO added. The $CF_3OC(O)O_2C(O)OCF_3$ concentration was routinely measured and accounted at most between 3% and 5% of the $CF_3OC(O)O_2NO_2$ reacted as will be shown later. All the products shown in the figure but $CF_3OC(O)O_2C(O)OCF_3$ have smaller absorption cross sections ($\sigma CF_3OC(O)O_2C(O)OCF_3 = 1.05 \times 10^{-17}$ cm^2 molecule^{-1} at 1133 cm^{-1}) [9]. The lower plot of the figure shows the residuals after subtraction of all the products formed. It is clear that there are no measurable or even identifiable species remaining.

The observed products can be quantitatively accounted for by a sequence of reactions following formation of the $CF_3OC(O)O_2$ radical as summarized in Table I. With respect to the model, the rate constant for formation of $CF_3OC(O)O_2C(O)OCF_3$ via recombination of CF_3OCOO was assumed to be similar to the CF_3O recombination and equals 1.4×10^{-11} cm^3 molecule^{-1} s^{-1} [14].

Table I Kinetic Model Used to Fit the Experimental Data

Reaction	Rate Constant[a]	Relative Sensitivity Coefficient (%)	References
$CF_3OC(O)O_2NO_2 + M \rightarrow CF_3OC(O)O_2 + NO_2 + M$	3.5×10^{-4}	92.3	This work
$CF_3OC(O)O_2 + NO_2 + M \rightarrow CF_3OC(O)O_2NO_2 + M$	6.6×10^{-12}	3.8	[11]
$CF_3OC(O)O_2 + NO \rightarrow CF_3OCOO + NO_2$	2.6×10^{-11}	3.8	[13]
$2\ CF_3OC(O)O_2 \rightarrow 2\ CF_3OCOO + O_2$	9.2×10^{-12}	<0.001	[13]
$2\ CF_3OCOO \rightarrow CF_3OC(O)O_2C(O)OCF_3$	1.4×10^{-11}	0.01	[14]
$CF_3OCOO \rightarrow CF_3O + CO_2$	40	0.02	This work
$CF_3O + NO \rightarrow CF_2O + FNO$	5.3×10^{-11}	0.04	[18]
$CF_3O + NO_2 \rightarrow CF_3ONO_2$	1.5×10^{-11}	0.04	[7]
$CF_3ONO_2 + HF \rightarrow CF_2O + FNO_2 + HF$	1×10^{-17}	<0.001	See text
$FNO \rightarrow HF + products$	>0.02	<0.001	[b]
$FNO_2 \rightarrow HF + products$	>0.002	<0.001	[b]

[a] First-order reactions, in s^{-1}; second-order reactions, in cm^3 $molecule^{-1}$ s^{-1}.
[b] The values reported correspond to lower limits to adjust for their disappearance.

The reaction leading to the unimolecular decarboxylation of CF_3OCOO:

$$CF_3OCOO \rightarrow CF_3O + CO_2 \qquad (7)$$

has been analyzed as part of a thorough study of the catalytic oxidation of CO to CO_2 mediated by CF_3O radicals at 298 K [15]. Measurements of the rate constant at different temperatures have not been reported. In this paper, we report a calculated value obtained through the fitting of the concentration–time profiles reported in that work for the trifluoromethoxycarbonyl peroxy nitrate and products experimentally determined at 298 K. This fit leads to a value of 40 s^{-1}, which is smaller than the values obtained by other workers. Other decarboxylation reactions have been studied, for example, by Maricq et al. [13,16], Wallington et al. [11], and Caralp et al. [6], who determined the rate constants for CF_3COO and C_6H_5COO radicals and concluded that the rate constants are significantly higher, around 5×10^4 s^{-1}. Our value for k_7 has to do mainly with the adjustment of the relative concentrations of CF_2O and $CF_3OC(O)O_2C(O)OCF_3$ and does not affect the kinetic parameters obtained for the thermal decomposition of the peroxy nitrate despite the difference with the value reported for decarboxylation of other radicals [6,11,13,16].

The NO added to the system efficiently captures the CF_3O radical via

$$CF_3O + NO \rightarrow CF_2O + FNO \qquad (8)$$

with a rate constant $k_8 = 5.3 \times 10^{-11}$ cm^3 $molecule^{-1}$ s^{-1} [18]. As can be seen in Fig. 1, CF_2O is clearly visible. In contrast, FNO could not be observed in the infrared spectra obtained, probably as a consequence of either its small infrared absorption cross section, or the fact that FNO molecules will react at the walls of our chamber with a lifetime much shorter (due to the size of our system) than the 10 min reported by other authors. This is consistent with the value used in the kinetic mechanism for the overall reaction that accounts for the disappearance of FNO.

In the system, the additional presence of NO_2 could lead to the formation of CF_3ONO_2 through reaction (9):

$$CF_3O + NO_2 \rightarrow CF_3ONO_2 \qquad (9)$$

with $k_9 = 1.5 \times 10^{-11}$ cm^3 $molecule^{-1}$ s^{-1} reported by Sander et al. [19]. In order for reaction (9) to reach a rate comparable to reaction (8), the NO_2 concentration would have to be more than three times the concentration of NO (unrealistic under our experimental conditions). Thus the inclusion of this reaction in the kinetic model corroborates that in our system CF_3ONO_2, if formed, is a very minor product and it should not be expected to lead to observable features in the IR spectra, especially if HF is present (see inset in Fig. 1) because it contributes to the catalytic decomposition of CF_3ONO_2 as reported by Sander et al. [20].

The possible cross-reactions between peroxy ($CF_3OC(O)O_2$) and oxy (CF_3OCOO, CF_3O) radicals would lead to the formation of the following two trioxides, $CF_3OC(O)O_3C(O)OCF_3$ and $CF_3O_3C(O)OCF_3$, respectively. The former has been synthesized and characterized for the first time in our laboratories [21], and the latter is a still unknown molecule. Despite the significant efforts done to look for IR features corresponding to trioxides, it is fairly clear that no indications of the presence of $CF_3OC(O)O_3C(O)OCF_3$ or any other trioxide are present in the residual spectrum

(see lower plot of Fig. 1). This is a consequence of the high NO_x concentrations present in the system. These reactions could become important in systems with very low or zero NO_x concentrations as Nielsen et al. reported [14] when they observed the formation of a trioxide in their system. Biggs et al. [22] considered secondary chemistry reactions since their concentrations of CF_3O_x and NO radicals differ by less than an order of magnitude.

The analysis presented above suggests, therefore, that the NO added to the system leads to the straightforward increase in NO_2 formation irrespective of the temperature, though the contribution is higher as the temperature rises. This increase in NO_2 could, in principle, affect the experimental determination of the rate of disappearance of peroxy nitrate via reaction (−1), and consequently lead to an error in the value of the rate constant for reaction (1). To consider and correct for this effect, two methods were applied.

The first is similar to that used by Christensen et al. [8] in the study of the thermal decomposition of $CF_3OC(O)O_2NO_2$ and was carried out for a temperature range between 283 and 303 K. The rate constant was corrected through the equation [8]

$$k_1 = k_{\text{obs}} \times (1 + (k_{-1} \times [NO_2])/(k_3 \times [NO])) \quad \text{(a)}$$

where k_{obs} corresponds to the observed rate of disappearance of $CF_3OC(O)O_2NO_2$, and $[NO_2]$ and [NO] to the concentrations of NO_2 and NO in the cell where the reaction was followed by infrared spectroscopy. In all cases, the correction was carried out taking into account the temperature dependence of the rate constants for reactions (−1) and (3).

The second method used was simulation at only one temperature (298 K) of the reaction progress through a kinetic model using the KINTECUS program available at www.kintecus.com [23]. The reactions considered for the model have been discussed above and, together with their corresponding rate constants, are collected in Table I. To check whether the rate constant measured in this paper will depend on the rates of reactions whose rate constants were taken from the literature (particularly, k_{-1} and k_2), a sensitivity analysis was carried out with the results shown in the third column of Table I. From the inspection of the relative sensitivity coefficients, it is clear that the only relevant contribution corresponds to the thermal decomposition reaction.

Figure 2 shows the fit to the concentrations of $CF_3OC(O)O_2NO_2$ and the products of the reaction for an experimental run conducted at room temperature. As can be seen, very good agreement between calculated and measured concentrations is reached for all the chemical species considered.

The two methods used gave no significant differences in the values obtained for the thermal decomposition of peroxy nitrate when analyzed at room temperature.

Before going deeper int the derivation of the activation energy for reaction (1), a brief explanation about the pressure dependence of the dissociation reaction should be given. $CF_3OC(O)O_2NO_2$ is a relatively big molecule having many degrees of freedom, and one should expect that the statistical limit to the redistribution of energy should be reached at relatively low pressures. To examine that expectation, a series of experimental runs were conducted at different total pressures and the decomposition of the peroxy nitrate recorded. Figure 3a shows the variation in concentration of the peroxy nitrate at 292 K measured at different

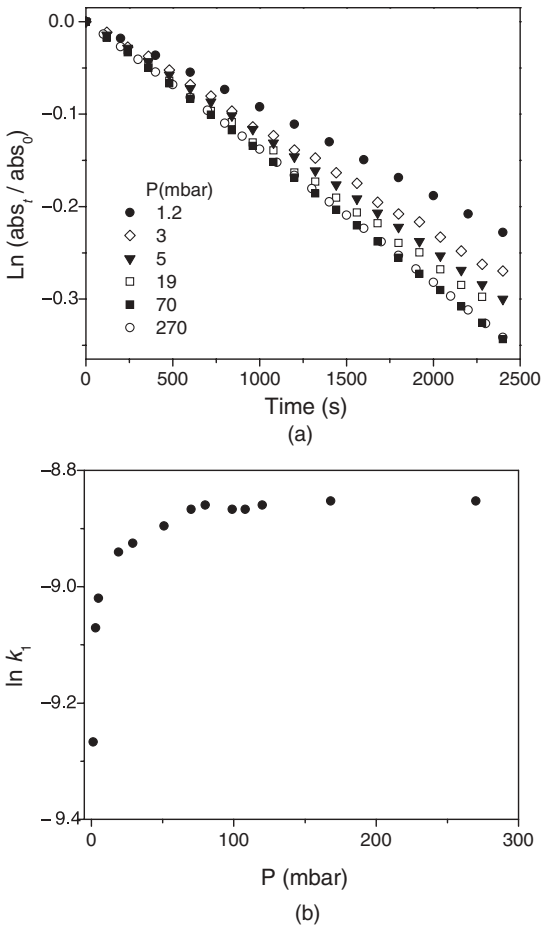

Figure 3 (a) Plot showing the disappearance of $CF_3OC(O)O_2NO_2$ at 292 K in the presence of NO at different total pressures monitored at 1760 cm^{-1}. Experiments carried out at pressures higher than 5 mbar were done by adding to the peroxy nitrate (usually, 0.7 mbar), NO (4.0 mbar), and He to reach the final reading. (b) Falloff curve at 292 K showing that at pressures higher than 70 mbar, k^{∞} is reached.

total pressures. As can be seen from the figure, studies at pressures higher than 70 mbar yield essentially the same global rate constant. This is further corroborated in panel (b) that shows measurements taken at closer pressure intervals in the 70–170 mbar range, presented in the plot as Ln k_1 versus pressure. Then, there is no significant dependence of the rate constant with pressures beyond the total value of 70 mbar. Nevertheless, our experimental runs used to derive the activation energy of the system were conducted at a total pressure of 270 mbar, ensuring that the kinetics studies were performed at the high-pressure limit. In this pressure range, the different constants were determined through the fitting, with a linear least-squares method, to at least 13 experimental points for each temperature.

The rate constants derived for the thermal decomposition of trifluoromethoxycarbonyl peroxy nitrate (reaction (1)) between 306 and 278 K are listed in Table II. The uncertainties in the rate constants presented in the last column correspond to one standard deviation of the linear least-squares regression obtained from the plot Ln[$CF_3OC(O)O_2NO_2$] versus time. Figure 4 shows the Arrhenius plot ($\mathrm{Ln}\,k = \mathrm{Ln}A - E_a/RT$) using the experimental data from Table II and leads to an extrapolated

Table II Rate Constants for the Thermal Decomposition of $CF_3OC(O)O_2NO_2$ at Different Pressures and Temperatures

		$k \times 10^{-5}$ (s^{-1})	
T (K)	Total Pressure (mbar)	Uncorrected	Corrected[a,b]
306	270.0	140	147 ± 3
302	270.0	73	77 ± 2
297	270.0	32.9	34.0 ± 0.5
293	270.0	17.9	18.4 ± 0.3
288	270.0	7.4	7.6 ± 0.1
284	270.0	4.11	4.2 ± 0.1
278	270.0	1.95	2.0 ± 0.1
292	270.0	13.9	14.3 ± 0.1
292	168.0	13.6	14.3 ± 0.1
292	120.0	13.8	14.2 ± 0.3
292	108.0	13.6	14.1 ± 0.1
292	99.0	13.7	14.1 ± 0.1
292	80.0	13.9	14.3 ± 0.2
292	70.0	13.7	14.1 ± 0.1
292	51.0	13.37	13.7 ± 0.1
292	29.0	12.99	13.3 ± 0.1
292	19.0	12.76	13.1 ± 0.1
292	5.0	11.8	12.1 ± 0.1
292	3.0	11.17	11.5 ± 0.1
292	1.2	9.26	9.4 ± 0.1

Uncorrected and corrected values using Eq. (a) are presented.

[a] Errors quoted for the rate constants correspond to one standard deviation of the linear least-squares regression.

[b] Corrected according to Eq. (a). See text.

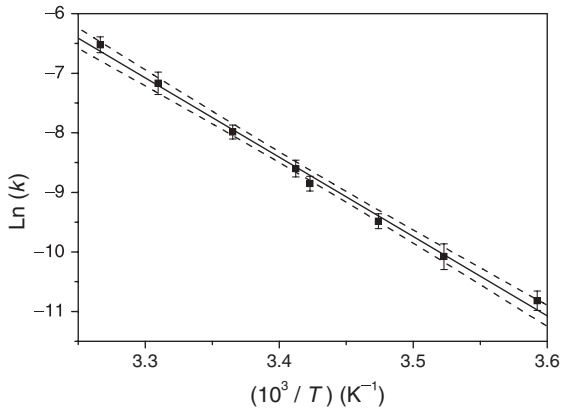

Figure 4 Arrhenius plot for k_1 from the corrected values given in Table II. The solid line represents the linear least-squares fit to the experimental points. Dashed lines represent the 95% confidence interval.

value of ($\mathrm{Ln}A = 37 \pm 1$) and an activation energy $E_a = (111 \pm 3)$ kJ mol^{-1}.

The rate constant at 296 K calculated from the Arrhenius plot, $k_1 = 2.5 \times 10^{-4}$ s^{-1}, very well agrees with the rate constant reported by Christensen et al. [8], $k_1 = 2.3 \times 10^{-4}$ s^{-1} at this temperature.

The derived kinetic parameters are also consistent with literature values for analogous reactions. Kirchner et al. [1], for example, reported that preexponential factors for substituted formyl peroxy nitrates range between 5×10^{15} and 1.6×10^{17} s^{-1}. These limits encompass our experimental value. Data reported for similar peroxy nitrates taken from the literature [1,4,6,11,24] are listed in Table III. As can be seen, all reported activation energies fall within a range of 9 kJ mol^{-1}. A closer inspection of the table shows that there is a systematic decrease in activation energy when an oxygen atom is present between the terminal and the carbonyl carbon atoms (compare rows 1 and 2, 3 and 4, and 5 and 6). This is in agreement with results obtained and reported by Caralp et al. [6]. It can also be seen that activation energies are larger for fluorinated counterparts (compare rows 1 and 3 and 2 and 4). This corroborates previous results [6] that suggest that fluorinated acyl peroxy nitrates are more stable than their nonfluorinated analogues.

Atmospheric Implications

The thermal lifetimes for the title compound as well as for PAN and FPAN have been calculated from the kinetic parameters presented in Table III. The results, gathered in Fig. 5, show the profile as a function of altitude and without any consideration about the changes of the rate constants with pressure. We noted earlier

Table III Kinetic Parameters for the Thermal Decomposition of Some Peroxy Nitrates (R-$OONO_2$)

R-	E_a (kJ mol^{-1})	A (10^{16})	T_i, T_f (K)	$k^{298} \times 10^4$ (s^{-1})	References
$CH_3C(O)$	112.9 ± 1.9	2.5	326–297	4.1 ± 0.2	[24]
$CH_3OC(O)$	107.0 ± 4.5	0.48	320–294	8.4	[4]
$CF_3C(O)$	116.4	1.9	303–285	0.75	[11]
$CF_3OC(O)$	111 ± 3	1.0	306–278	3.50 ± 0.05	This work
$C_6H_5C(O)$	113.1	2.1	322–293	3.1	[6]
$C_6H_5OC(O)$	112.7 ± 7.7	3.0[a]	316–302	0.53	[1]
t-$C_4F_9OC(O)$	111.6 ± 4.7	4.5	308–293	12.1	[4]

[a] Assumed as typical values for acyl nitrates in Kirchner et al. [1].

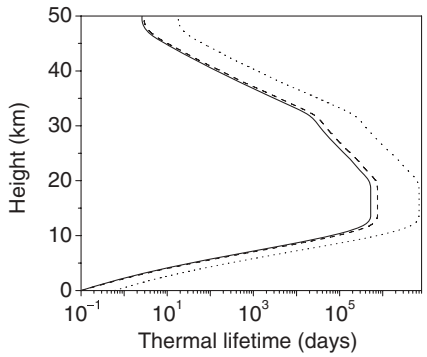

Figure 5 Atmospheric thermal lifetime of $CF_3OC(O)O_2NO_2$ uncorrected for pressure dependence as measured in this work (solid line). PAN (dashed line) and FPAN (dotted line) are plotted for reference and were taken from literature data.

that our measurements show pressure dependence below 270 mbar; that is, we should expect modifications from 18 km up. For these reasons, the figure must be interpreted only as a trend for altitudes above the tropopause. Irrespective of the pressure dependence, the figure depicts features for $CF_3OC(O)O_2NO_2$ and PAN that are similar throughout the entire range of altitudes. This suggests that once $CF_3OC(O)O_2NO_2$ is formed in the atmosphere, it could transport NO_2 radicals with the same efficiency as PAN and other peroxy nitrates that have been spectroscopically shown to be present.

The figure also shows the profile of FPAN, and it is clearly seen the influence of the fluorine substitution on the generated (PAN) molecule yielding a longer lifetime throughout.

MDM is a grateful recipient of a CONICET fellowship.

BIBLIOGRAPHY

1. Kirchner, F.; Mayer-Figge, A.; Zabel, F.; Becker, K. H. Int J Chem Kinet 1999, 31, 127–144.
2. Ko, M. K. W.; Sze, N. D.; Rodriguez, J. M.; Weistenstein, D. K.; Heisey, C. W.; Wayne, R. P.; Biggs, P.; Canosa-Mas, C. E.; Sidebottom, H. W.; Treacy, J. Geophys Res Lett 1994, 21, 101–104.
3. Talukdar, R. K.; Burkholder, J. B.; Schmoltner, A. M.; Roberts, J. M.; Wilson, R. R.; Ravishankara, A. R. J Geophys Res, [Atmos] 1995, 100(14), 163–173.
4. Kirchner, F.; Thuener, L. P.; Barnes, I.; Becker, K. H.; Donner, B.; Zabel, F. Environ Sci Technol 1997, 31, 1801–1804.
5. Atkinson, R.; Aschmann, S. M.; Winer, A. M.; Carter, W. P. L. Atmos Environ 1984, 18, 2105–2107.
6. Caralp, F.; Foucher, V.; Lesclaux, R.; Wallington, T. J.; Hurley, M. D. Phys Chem Chem Phys 1999, 1, 3509–3517.
7. von Ahsen, S.; Garcia, P.; Willner, H.; Argüello, G. A. Inorg Chem 2005, 44, 5713–5718.
8. Christensen, L. K.; Wallington, T. J.; Guschin, A.; Hurley, M. D. J Phys Chem A 1999, 103, 4202–4208.
9. Argüello, G. A.; Willner, H.; Malanca, F. E. Inorg Chem 2000, 39, 1195–1199.
10. Zabel, F.; Kirchner, F.; Becker, K. H. Int J Chem Kinet 1994, 26, 827–845.
11. Wallington, T. J.; Sehested, J.; Nielsen, O. J. Chem Phys Lett 1994, 226, 563–569.
12. Tyndall, G. S.; Cox, R. A.; Granier, C.; Lesclaux, R.; Moortgat, G. K.; Pilling, M. J.; Ravishankara, A. R.; Wallington, T. J. J Geophys Res, [Atmos] 2001, 106, 12157–12182.
13. Maricq, M. M.; Szente, J. J.; Khitrov, G. A.; Francisco, J. S. J Phys Chem 1996, 100, 4514–4520.
14. Nielsen, O. J.; Ellermann, T.; Sehested, J.; Bartkiewicz, E.; Wallington, T. J.; Hurley, M. D. Int J Chem Kinet 1992, 24, 1009–1021.
15. Burgos Paci, M. A.; Arguello, G. A. Chem Eur J 2004, 10, 1838–1844.
16. Maricq, M. M.; Szente, J. J.; Dibble, T. S.; Francisco, J. S. J Phys Chem 1994, 98, 12294–12309.
17. Malanca, F. E.; Argüello, G. A.; Staricco, E. H.; Wayne, R. P. J Photochem Photobiol A Chem 1998, 117, 163–169.
18. Atkinson, R.; Baulch, D. L.; Cox, R. A.; Crowley, J. N.; Hampson, R. F., Jr.; Kerr, J. A.; Rossi, M. J.; Troe, J. IUPAC Subcommittee on Gas Kinetic Data Evaluation for Atmospheric Chemistry Web Version 2001, 1–56. http://www.iupac-kinetic.ch.cam.ac.uk

19. Sander, S. P.; Friedl, R. R.; Ravishankara, A. R.; Golden, D. M.; Kolb, C. E.; Kurylo, M. J.; Huie, R. E.; Orkin, V. L.; Molina, M. J.; Moortgat, G. K.; Finlayson-Pitts, B. J. Chemical Kinetics and Photochemical Data for Use in Atmospheric Studies. Evaluation number 14; Jet Propulsion Laboratory, Pasadena, CA, 2005.
20. Sander, S.; Willner, H.; Oberhammer, H.; Argüello, G. A. Z Anorg Allg Chem 2001, 627, 655–661.
21. von Ahsen, S.; Garcia, P.; Willner, H.; Paci, M. B.; Argüello, G. A. Chem Eur J 2003, 9, 5135–5141.
22. Biggs, P.; Canosa-Mas, C. E.; Fracheboud, J. M.; Percival, C. J.; Wayne, R. P.; Shallcross, D. E. J Chem Soc, Faraday Trans 1997, 93, 379–385.
23. Ianni, J. C. KINTECUS, Windows version 2004, 3.7.
24. Bridier, I.; Caralp, F.; Loirat, H.; Lesclaux, R.; Veyret, B.; Becker, K. H.; Reimer, A.; Zabel, F. J Phys Chem 1991, 95, 3594–3600.